https://doi.org/10.5194/bg-2020-13
Preprint. Discussion started: 3 March 2020

Biogeosciences Discussions
Open Access
EGU

Modelled potential forest area in the forest-steppe of central Mongolia is about three times of actual forest area

Michael Klinge[1]*, Choimaa Dulamsuren[2], Florian Schneider[1], Stefan Erasmi[3], Markus Hauck[2], Uudus Bayarsaikhan[4], Daniela Sauer[1]

[1] Department of Physical Geography, Institute of Geography, University of Göttingen, Goldschmidtstraße 5, 37077 Göttingen, Germany

[2] Applied Vegetation Ecology, Faculty of Environment and Natural Resources, University of Freiburg, Tennenbacher Str. 4, 79106 Freiburg, Germany

[3] Department of Cartography, GIS and Remote sensing, Institute of Geography, University of Göttingen, Goldschmidtstraße 5, 37077 Göttingen, Germany

[4] Department of Biology, School of Arts and Sciences, National University of Mongolia, Baga toiruu 47, Sukhbaatar duureg, Ulaanbaatar, Mongolia

* corresponding author: mklinge1@gwdg.de

Keywords: Tree biomass, forest-steppe, forest fire, permafrost, Mongolia

Abstract

The Mongolian forest-steppe is highly sensitive to climate change and environmental impact. The intention of this study was to identify, which geoecological parameters control forest distribution and tree growth in this semi-arid environment, and to evaluate the actual and potential tree biomass. For this purpose, we applied a combination of tree biomass and soil mapping, remote sensing and climate data analysis to a study area in the northern Khangai Mountains, central Mongolia.

Forests of different landscape units and site conditions generally showed minor differences in tree biomass. We found no significant correlation between tree biomass and NDVI (normalized differentiated vegetation index). Tree biomass was reduced at forest edges, in small fragmented

https://doi.org/10.5194/bg-2020-13
Preprint. Discussion started: 3 March 2020

forest stands of the steppe-dominated area, and in large forest stands, compared to all other forest units. The tree biomass of forests on slopes ranged between 25 and 380 Mg ha^{-1}. The mean tree biomass in forests of 10-500 ha was 199-220 Mg ha^{-1}, whereby tree biomass at the forest edges was 50-63 Mg ha^{-1} less than in the interior parts of the forests. The mean tree biomass of forests >500 ha was 182 Mg ha^{-1}, whereas that of forests <10 ha in the steppe-dominated area was only around 142 Mg ha^{-1}. Forests in alluvial plains had maximum tree biomasses of 440-688 Mg ha^{-1}. In contrast to tree biomass, the spatial extension of forests showed distinct relationships with topographic and climatic parameters. Presence of forest was controlled by elevation (<2600 m a.s.l.), aspect (no southern slopes below 2100 m a.s.l.), slope (<25°), mean annual precipitation (160-340 mm) and mean growing season temperature (6.5-10.8 °C).

The actual forests of the study area covered 1,086 km^2. In 1986, prior to extensive forest fires, it was 1,898 km^2. The actual tree biomass of 20 x10^9 g represented 57 % of that in 1986. Modelling of the potential forest area resulted in 3,552 km^2, with 65 x10^9 g tree biomass (based on topographic parameters) and 3,113 km^2 with 58 x10^9 g tree biomass (based on climatic parameters), respectively. The modelled potential forest area was thus about three times the actual forest area.

1. Introduction

The Mongolian forest-steppe represents the transition zone between the southern limit of the boreal forest in Central Asia and the dry region of the Gobi Desert. This ecotone has semi-arid climate and is highly vulnerable to climate change and land-use intensification (Poulter et al., 2013; Yang et al., 2016; Khansaritoreh et al., 2017). Various ecological stress factors have recently reduced Mongolia's forest area and thus, most likely tree biomass as well (Dulamsuren et al., 2008; 2010a; 2010c). Drought stress and resulting decline in wood production and forest regeneration were repeatedly reported, especially for Siberian larch (*Larix sibirica,* Ledeb.), which makes up approximately 80 % of the total forest area (Dulamsuren et al., 2010b; Dulamsuren et al., 2014; Liu et al., 2013; Dulamsuren et al., 2009; Dulamsuren et al., 2010a; Hauck et al., 2019). Mongolia's mean annual air temperature has increased by 0.27 K per decade (or absolutely 1.7 K) from 1940 to 2001 (Batima et al., 2005),

https://doi.org/10.5194/bg-2020-13
Preprint. Discussion started: 3 March 2020

which is clearly above the global average of 0.12 K per decade from 1951 to 2012 (IPCC, 2013). In addition, hazardous forest fires destroyed large forest areas in Mongolia over the last decades (Goldammer, 2002; Nyamjav et al., 2007; Hansen et al., 2013). Furthermore, the lack of a systematic forest management, insufficient control of logging and forest pasture in the vicinity of grasslands contributed to the degradation and reduction of forests (Tsogtbaatar, 2004; Dulamsuren et al., 2014).

Boreal forests represent an important organic carbon pool and are thus important for the global climate (Pan et al., 2011; Goodale et al., 2002). Although most of the organic carbon in the boreal zone is stored in the soil (Deluca and Boisvenue, 2012; Mukhortova et al., 2015; Shvidenko and Schepaschenko, 2014), a considerable amount of carbon is also stored in the tree biomass. Typically, carbon stocks in the tree biomass of boreal forests range from 40 to 80 Mg C ha^{-1} (Thurner et al., 2014; Jarvis et al., 2001; Luyssaert et al., 2007). Extensive forest use, fire-setting, and woodcutting has reduced the forest area and tree biomass in Central Asia since prehistoric times (Miehe et al., 2007; Unkelbach et al., 2019; Unkelbach et al., 2017). Its impact can be evaluated by estimating the potential extent of forest area based on climatic and topographic parameters (Klinge et al., 2015).

Investigations on tree biomass in the Mongolian forest-steppe have been carried out in the Altai Mountains, southern Khangai Mountains (Dulamsuren et al., 2016), northern Khangai Mountains (Dulamsuren et al., 2019), and Khentei Mountains (Danilin and Tsogt, 2014). Tree biomass reported from these studies ranged between 123 and 397 Mg ha^{-1}. Average tree biomass tends to decrease from the more humid north to the arid south. At local scale, tree biomass in the interior of *Larix sibirica* forests exceeds that at the forest edges (Dulamsuren et al., 2016). No consistent significant differences in tree biomass were found between forest-stands of varying sizes and between forests growing in grassland- and forest-dominated areas of the forest-steppe ecotone (Dulamsuren et al., 2019).

Various methods have been established to quantify tree biomass by relating field measurements with remote sensing data. However, all these methods come with specific errors (Rodríguez-Veiga et al., 2017; 2019; Lu et al., 2015; Powell et al., 2010). The main limitation of vegetation indices from multispectral satellite images, such as the NDVI (normalized differentiated vegetation index), is that the signal becomes saturated, when the upper leaves cover lower leaves of the tree canopy layer. The mean crown closure of Mongolian forests is 0.53 (Goldammer, 2007), which suggests that the NDVI should be applicable in the study area. Dulamsuren et al. (2016) interpolated the tree biomass and carbon stock of entire Mongolia based on Spot-NDVI and field data. Thurner et al. (2014) used a growing stock volume product from synthetic aperture radar data to estimate the tree density and carbon stock of boreal and temperate forests of the northern hemisphere.

Beside biomass estimation, the NDVI has often been used to analyse vegetation dynamics in response to climatic shifts (Buermann et al., 2014; Miao et al., 2015; Poulter et al., 2013; Vandandorj et al., 2015). However, delineating vegetation trends from vegetation indices must be done with caution, because these parameters strongly depend on the spatial resolution and the recording season of the satellite image. Moreover, indices like the NDVI include a mixture of greenness signals from different vegetation types. Karnieli et al. (2013) gave an example for the problems in interpreting vegetation degradation in a case study on Mongolian pastures.

The parameters precipitation, temperature and evaporation control the spatial pattern of forest and steppe distribution in the semi-arid forest-steppe (Klinge et al., 2018; Nyamjav et al., 2007; Dulamsuren and Hauck, 2008). In addition, topographic position plays an important role, as forests are strictly limited to north-facing slopes (Klinge et al., 2015; Hais et al., 2016). Thus, relief is an important factor for the existence, vitality and tree density of forests. In addition to natural factors, the actual forest distribution is strongly influenced by human impact, which exists since prehistoric times (Miehe et al., 2007), and by intense forest fires that occurred during the last decades.

Based on the state of knowledge described above, we addressed the following hypotheses:

(I) The actual tree biomass in the study area depends on soil conditions and topographic position and has been strongly reduced by forest fires and logging.

(II) The NDVI is a suitable parameter for tree biomass assessment in the study area.

https://doi.org/10.5194/bg-2020-13
Preprint. Discussion started: 3 March 2020

(III) Tree vitality depends on ecological site conditions, whereas climate and topography are the main limiting factors for the distribution of larch forests in the study area (to be deduced by spatial analysis of climatic and topographic data).

(IV) The potential forest area and tree biomass are much larger than the actual ones.

We aimed at answering the following research questions:

- What are the general climatic and ecological limitations for forest distribution in the mountain forest-steppe (to be deduced by GIS and remote sensing analysis)?
- Is there an influence of soil conditions, forest use and fire events on tree biomass, depending on forest fragmentation and stand size?
- How large are the losses of forest area and tree biomass due to recent forest fires in the study area?
- How large are the potential forest area and tree biomass in the study area?

2. Study area

The study area is located on the northern slopes of the Khangai Mountains near the town Tosontsengel in northern central Mongolia (98°16'E/48°46'N) (Fig. 1). The region has continental climate with cold semi-arid conditions (Figure 2). The monthly mean temperatures at Tosontsengel range between -31.7 °C in January and 14.7 °C in July. Most of the annual precipitation occurs during summer, from low pressure cells brought by the westerlies (Batima et al., 2005). In contrast, the Siberian high during winter causes mostly dry conditions. The cold climate promotes discontinuous permafrost, with permafrost mainly occurring in the valley bottoms, on the upper mountains, and partially on the slopes. The existence of permafrost ice requires some soil moisture, whereas dry soil conditions lead to dry permafrost, i.e., frozen ground without ice.

The maximum altitudes of up to 3,200 m a.s.l. lie in the southern part of the study area. They are characterised by mountain plateaus with cryoplanation terraces (Kowalkowski and Starkel, 1984; Richter et al., 1963). These highest regions belong to the periglacial belt, where alpine vegetation and bare, rock-debris covered land surfaces occur above the upper treeline at approx. 2,500 m a.s.l.

https://doi.org/10.5194/bg-2020-13
Preprint. Discussion started: 3 March 2020

(Klinge et al., 2018). In the northern part, the mountains are lower, and mountain forest-steppe covers the north-facing slopes up to the summits. The main valleys run from south to north, leading into the east-west running valley of the Ider Gol (Gol = River) at an elevation of 1,600 m a.s.l. The geological basement consists of Permian metamorphosed sedimentary and acid plutonic rock, and Carboniferous mafic rock (Academy of Sciences of Mongolia and Academy of Sciences of USSR, 1990). Coarse detritus of these bedrocks builds up the slope debris, which is often mixed with and covered by sandy to silty aeolian deposits.

Dense, extensive forests occur south of the Ider Gol, whereas in the north, forests are more fragmented and steppe vegetation is dominant (Dulamsuren et al., 2019). A clear spatial pattern of forests (made up of *Larix sibirica*) on the northern slopes and steppe on the southern slopes is typical in the forest-steppe of Mongolia (Hilbig, 1995; Treter, 1996). This vegetation pattern is generally controlled by low precipitation (<300 mm), high evapotranspiration and relief-controlled differences in insolation in the mid-latitudes (Hais et al., 2016; Schlütz et al., 2008). Riverine forests consist of willow (*Salix*), poplar (*Populus*), and larch (*Larix sibirica*). Since these alluvial forests are supported by groundwater, they are more independent from the local precipitation. Pleistocene dune fields with scattered individual old larch trees are abundant in the basins. There are many local forest and steppe fires during the summer season (Goldammer, 2007; Hessl et al., 2012). Hazardous forest fires in 1996 and 2002 destroyed extensive forests. Many of these former forest areas have not yet regrown.

A timber factory and forest tracks were established in the Tosontsengel region during Soviet times to facilitate intensified forest exploitation since the 1960s. Industrial logging was abandoned after the political change in the early 1990s, but has been partly resumed. In addition, the local population extracts fuelwood from the forests.

https://doi.org/10.5194/bg-2020-13
Preprint. Discussion started: 3 March 2020

Biogeosciences
Discussions

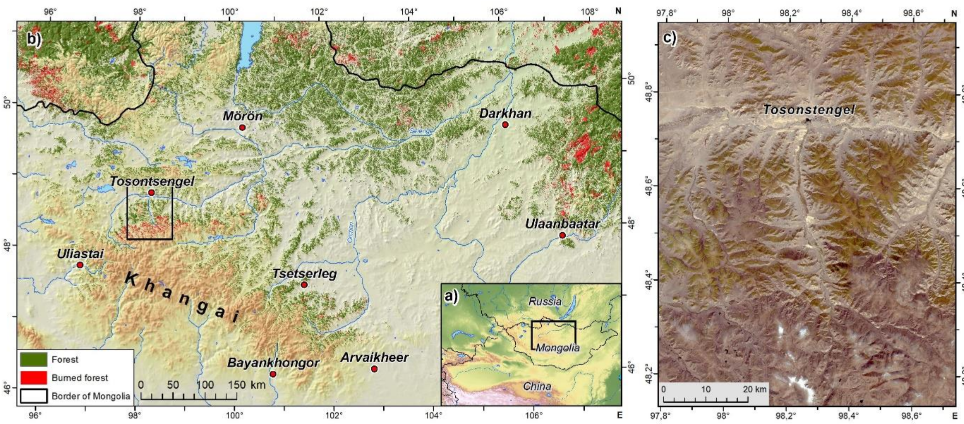

Figure 1: Study area. a) Overview of Mongolia with position of the map shown in b) (black frame). b) Location of the study area in the forest-steppe of northern central Mongolia. The forest distribution was adapted from Klinge et al. (2018), whereas the burnt forest area (2000-2018) was mapped by Hansen et al. (2013). The digital elevation model (DEM) was created from SRTM (Shuttle Radar Topography Mission) data. The black frame in b) indicates the position of the image shown in c). c) True colour satellite image of the study area near Tosontsengel (Landsat 8, September 22, 2014).

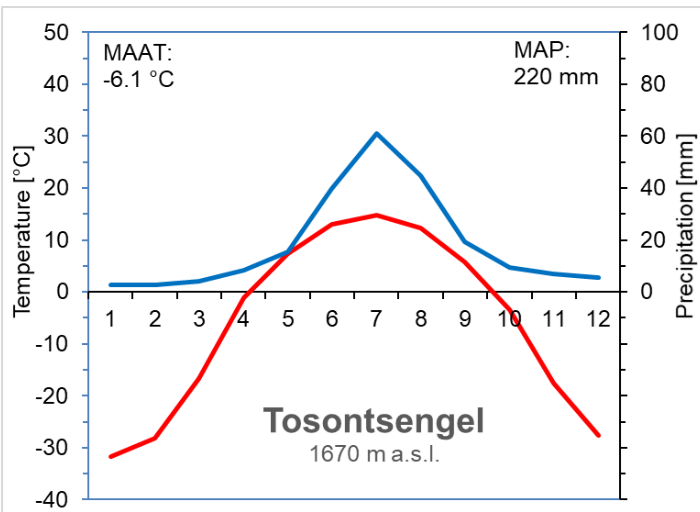

Figure 2: Climate diagram for Tosontsengel (measuring period 1968-2013).

3. Methods

https://doi.org/10.5194/bg-2020-13
Preprint. Discussion started: 3 March 2020

3.1. Tree biomass measurements and site mapping

During fieldwork in the years 2014-2018, we determined the tree biomass on 20 m x 20 m plots, by measuring the tree diameter at breast height (dbh) and tree height for all trees exceeding a height of 4 m. We used either a Vertex IV ultrasonic clinometer and T3 transponder (Haglöf, Långsele, Sweden) or a True Pulse 200 laser rangefinder (Laser Technology, Inc., USA) for measuring tree height. Stem diameter was calculated from stem circumference as measured with a measuring tape. In this way, we analysed 140 plots, in order to cover forest- and steppe-dominated landscapes, forest edge and interior, toe slope, mid-slope, upper slope, natural and exploited forests, as well as different aspects and forest-stand sizes. We applied the two allometric functions for Siberian larch (*Larix sibirica*) in Mongolia published by Battulga et al. (2013) and Dulamsuren et al. (2016), and used the mean of the results of both equations to estimate the aboveground and belowground tree biomass. Differences in the estimates of the two functions are discussed in Dulamsuren et al. (2016). Forest stands where tree stumps indicated woodcutting, were mapped as forests with "logging", whereas forest stands without tree stumps were mapped as forests with "no logging". Forest stands, where burned bark and/or charred wood indicated former fire events, were mapped as having "fire indicators", those without as having "no fire indicators". Ground vegetation structure, soil profiles and detection of permafrost provided auxiliary data. In 24 tree biomass plots, we measured the Leaf Area Index (LAI) using a LI-COR Plant Canopy Analyzer LAI-2200 C (Licor Biosciences, USA).

3.2. Remote sensing analysis of forest distribution

The workflow of the digital forest-distribution analysis, including input, intermediate and output data, is illustrated in Figure 3. We used a supervised classification of a Landsat 5 satellite image from September 23, 1986 to delineate the forest distribution before the extensive fires. We determined the actual forest area (AFA) by integrating supervised image classifications from several scenes of Landsat 8 (May 14, 2013; June 20, 2015) and Sentinel 2 (Sep 14, 2016; Sep 19, 2017) to receive the best possible forest representation. The difference in forest area between the images of 1986 and 2017 represents the burnt forest area (BFA) for this period.

https://doi.org/10.5194/bg-2020-13
Preprint. Discussion started: 3 March 2020

We used a digital elevation model (DEM) based on TanDEM-X data to compute various topographic parameters (see Figure 3), in order to identify possible relationships between tree biomass and relief. Due to the high horizontal (10 x 10 m) and vertical (<1 m) resolution of the DEM, the calculated terrain surface was distorted by the forest canopy, especially at the edges of the forest stands. Thus, we used the AFA map obtained from the satellite image classification for correcting the DEM in the forest areas. In addition, we created NDVI maps from Landsat 5/8 and Sentinel 2 multispectral images to determine the vitality of the vegetation and to test potential correlations between the NDVI and tree biomass estimations. The classification of different landscape units (LU) was based on (1) the proportion between forest and steppe areas, distinguishing forest-dominated area (FDA) and steppe-dominated area (SDA), (2) the position of the upper treeline in the high mountain area (HMA), (3) flat area (<2°) in the alluvial plains and (4) dunes, identified based on multispectral satellite images.

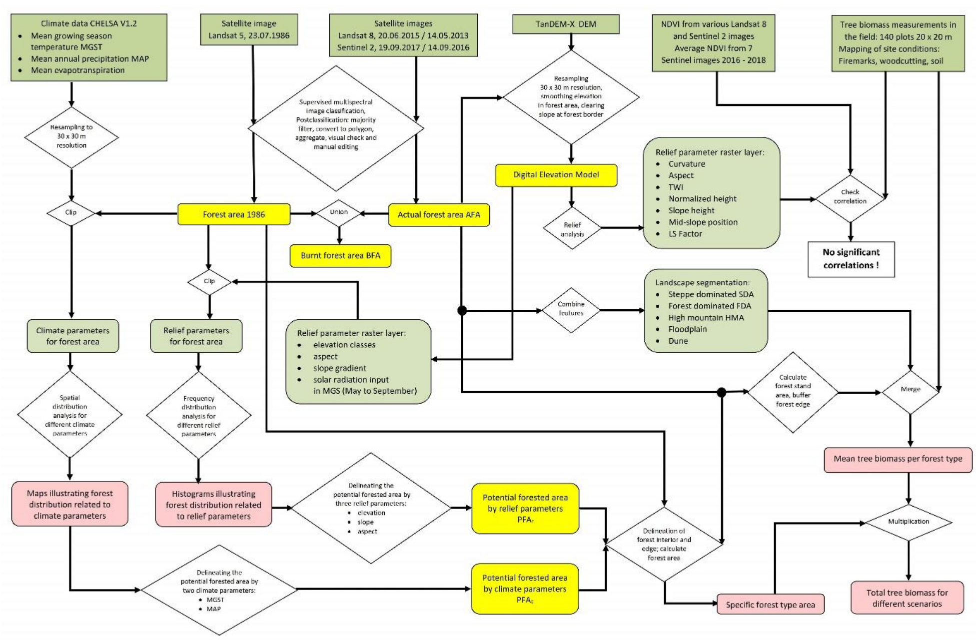

Figure 3: Workflow of the forest-distribution and tree biomass GIS analysis.

https://doi.org/10.5194/bg-2020-13
Preprint. Discussion started: 3 March 2020

We applied the approach of Klinge et al. (2015) to identify the potential forest area (PFA) based on relief parameters. For this purpose, we used the forest area in 1986 to identify the relationships between relief and forest distribution, considering elevation, aspect, slope, and insolation during the mean growing season (MGS, May-September). We chose the forest status of 1986 for the statistical analysis, because at that time, forest distribution was still less disturbed by forest fires than today.

In addition, we performed a forest distribution analysis based on the climatic parameters mean annual precipitation (MAP), mean growing season temperature (MGST; mean of the monthly mean temperatures between May and September), and mean annual potential evaporation. For this purpose, we used climate data from the CHELSA V1.2 dataset (Karger et al., 2018), which we resampled from the originally 30-arcsec resolution to obtain 30 m resolution. In this reanalysed climate dataset, we also considered terrain parameters and wind effect, in order to obtain an improved representation of climate conditions in relief terrain (Karger et al., 2017). We calculated MAP and MGST for the period 1973-2013. In addition, we applied a GIS-tool on TanDEM-X data to estimate the cumulative insolation for the period Mai-September 2017, which served as an example for the mean growing season.

Finally, we delineated three different forest distribution patterns, namely the actual forest area (AFA), the forest area of 1986, and the potential forest area (PFA). The forest areas were assigned to five different landscape units, namely steppe-dominated area (SDA), forest-dominated area (FDA), high-mountain area (HMA), alluvial forest, and dune. We distinguished four forest-size classes (FSC): F1, G1 = <0.1 km^2 in the forest-dominated and steppe-dominated areas, respectively; F2 = 0.1-1 km^2; F3 = 1-5 km^2; F4 = >5 km^2 and used a spatial buffer of 30 m to distinguish the forest edges from the interior. These classification schemes were adapted from Dulamsuren et al. (2016; 2019).

3.3. Classification of site conditions

Dulamsuren et al. (2019) already analysed the interior of larch forests on slopes in the same study area, thereby focusing on larch stands in the optimum stage of the forest development cycle (Jacob et al., 2013; Feldmann et al., 2018) and excluding recent heavy disturbances like severe fire or clear-

https://doi.org/10.5194/bg-2020-13
Preprint. Discussion started: 3 March 2020

Biogeosciences Discussions
Open Access
EGU

cut. Complementary to that study, we included larch stands with varying site conditions, history and structure, in order to assess tree biomass variability in response to disturbances and site conditions. In this way, we also tested the sensitivity of tree biomass to varying specific site conditions and thus the potential of remote sensing techniques for upscaling plot-based data to the landscape level. We therefore used the tree biomass data from the 30 *L. sibirica* plots on slopes of Dulamsuren et al. (2019) and added tree biomass data from forest edges and further *L. sibirica* plots of different stand sizes (classes F1/G1 to F4) and forest-to-grassland ratios (FDA with classes F1 to F4 vs. SDA with class G1). In addition to these forests on slopes, we also analysed larch forests on alluvial sands in floodplains. However, their limited size did not allow to obtain separate datasets for forest interior and edge. Altogether, we distinguished 12 larch-stand types, including forest interior and forest edges of the slope forest types F1, F2, F3, F4 and G1, and the floodplain forests as independent variables, and differentiating between logged / not logged and burned / not burned forest stands as covariates, based on the presence / absence of tree stumps and fire scars.

We calculated the mean tree biomass for each site-condition class such as wood harvest, fire indicators, and topsoil conditions (Table 1), checked the tree biomass data of each class for normal distribution and tested the differences between the tree biomass data for the various site conditions for statistical significance using Duncan's multiple range test of the SPSS software package. The relationships between tree biomass, NDVI and terrain parameters were statistically analysed by Pearson correlations to identify the best interpolation strategy for the forest distribution and tree biomass of 1986 and PFA. However, we found only weak correlations between tree biomass and NDVI, (see results chapter). Thus, finally, we delineated the various forest types with their specific tree biomass (with respect to the AFA, BFA and PFA) by multiplying the area of each forest type with the mean tree biomass value of that forest type. A delineation of potential alluvial forests was not feasible, because the erosion-deposition dynamics of the braided rivers control the geomorphological landscape development and thus the distribution of alluvial plains and related forests.

https://doi.org/10.5194/bg-2020-13
Preprint. Discussion started: 3 March 2020

Biogeosciences Discussions
Open Access

4. Results

4.1. General patterns of forest fire and permafrost distribution

The actual forest area (AFA), subdivided into four size classes, and the burnt forest area (BFA) are presented in Figure 4. We found only few burnt areas in the steppe-dominated areas (SDA) in the north-western and eastern parts of the study area. In the forest-dominated (FDA) central and north-eastern parts of the study area, the most extensive burned forest areas (BFA) were in the upper mountains. The high mountain area (HMA) in the southern part had lost the largest portion of forest by fire. Its formerly large forest areas had turned into numerous small and fragmented forest remnants.

Our soil profiles showed that among the large forest stands on the slopes, permafrost was restricted to the FDA and HMA. Under large forest stands (forest size class F4) on north-facing slopes, the permafrost was rich in ice and occurred already at shallow depth, whereas east- and west-facing slopes had only small patches of permafrost that started at depths of more than 1 m. The frozen ground contained only little ice, where sandy materials made up the upper parts of the soils. There was no field evidence for permafrost under fragmented forest stands (G1, F1, F2) and burnt forests.

4.2. Plot-based tree biomass data

The mean tree height in the plots ranged between 12 and 20 m, whereas the maximum heights of single trees reached up to 32.7 m. The stand densities were between 5 and 91 m^2 ha^{-1}, with an average stand density of 38.8 m^2 ha^{-1}. The mean tree ages were determined between 100 and 200 years, whereas maximum tree ages up to 380-413 years were found. Tree biomass in the larch forests on slopes ranged between 25 Mg ha^{-1} and 380 Mg ha^{-1}. Maximum tree biomasses of 440-688 Mg ha^{-1} were found in floodplain forests, whereas larch trees on sand dunes only formed open woodlands with less tree biomass (48 Mg ha^{-1}, n=1). Mean tree biomasses for the various forest-stand sizes and ecological parameters (Fig. 3), are listed in Table 1. Variance analyses did not proof statistically significant differences between the forest classes (Figure 5). Forests of the size classes F1, F2, and F3 had 50-63 Mg ha^{-1} less tree biomass at forest edges than in the interiors. The small

https://doi.org/10.5194/bg-2020-13
Preprint. Discussion started: 3 March 2020

fragmented forests G1 in the SDA had up to 70 Mg ha^{-1} less tree biomass than those in the FDA. Logging, forest fire and material making up the upper parts of the soils did not have any distinct influence on tree biomass. The large proportion of forest with wood harvest in the small fragmented forests (size classes F1 and G1) pointed to the strong exploitation pressure on these forest types. In all stand-size classes of the FDA forests, the tree-biomass means and medians lay within 180-220 Mg ha^{-1}. The maximum tree biomass was more than 320 Mg ha^{-1}. The forest-size class F4 showed no distinct difference in tree biomass between forest edges and interior.

https://doi.org/10.5194/bg-2020-13
Preprint. Discussion started: 3 March 2020

297

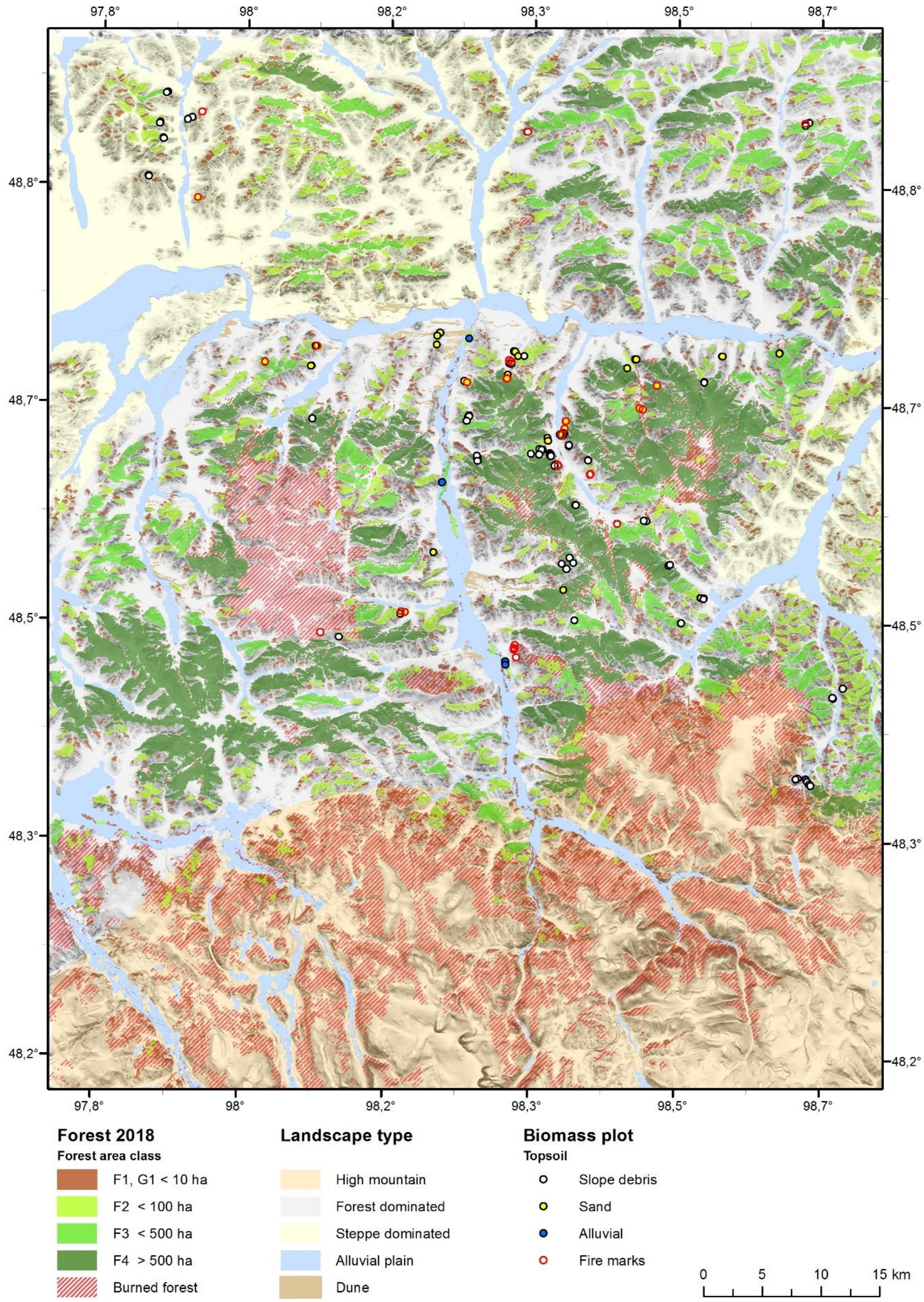

298 *Figure 4: Landscape types in the study area, with actual forest area (AFA) and burnt forest area (BFA)*

299 *(reference year 2018). The shaded relief illustration is based on TanDEM-X data.*

https://doi.org/10.5194/bg-2020-13
Preprint. Discussion started: 3 March 2020

Table 1: Mean tree biomass (above and belowground) for different forest types and site conditions. Plots, where site conditions could not unambiguously be identified, were excluded from the corresponding analysis part. SE = standard error, n = number of plots.

	F1	SE	*n*	F2	SE	*n*	F3	SE	*n*	F4	SE	*n*	G1	SE	*n*
total	**198.7**	11.2	*29*	**208.0**	11.8	*31*	**212.5**	13.9	*31*	**182.0**	12.9	*34*	**142.2**	10.7	*10*
forest interior	219.3	14.0	*18*	218.2	12.6	*26*	220.6	13.4	*26*	181.7	13.8	*30*	145.4	15.0	*7*
forest edge	165.1	13.7	*11*	155.2	21.0	*5*	170.7	46.2	*5*	184.3	35.2	*4*	134.8	2.7	*3*
difference	54.2			63.0			49.9			-2.6			10.6		
no fire indicators; no logging	211.5	22.3	*2*	210.7	18.1	*5*	219.0	12.8	*4*	170.7	14.3	*15*			
no fire indicators	204.8	18.7	*14*	206.2	12.8	*14*	194.3	17.4	*21*	168.3	13.3	*23*	122.1	2.7	*2*
fire indicators	179.5	15.2	*9*	171.6	20.9	*11*	231.3	14.4	*6*	175.5	39.7	*5*	154.9		*1*
difference	25.2			34.6			-36.9			-7.2					
no logging	211.5	22.3	*2*	234.3	11.9	*8*	238.8	23.8	*6*	180.4	13.7	*18*	134.1	4.0	*2*
logging	197.8	11.9	*27*	198.9	14.4	*23*	207.4	16.6	*24*	183.8	22.7	*16*	144.3	13.2	*8*
difference	13.7			35.4			31.4			-3.4					
slope debris	211.0	18.4	*13*	207.8	16.5	*18*	196.3	18.5	*19*	176.7	14.3	*28*			
sand layer	188.8	13.3	*16*	204.5	15.8	*14*	238.3	18.3	*12*	214.4	24.5	*7*			
difference	22.2			3.4			-42.0			-37.7					

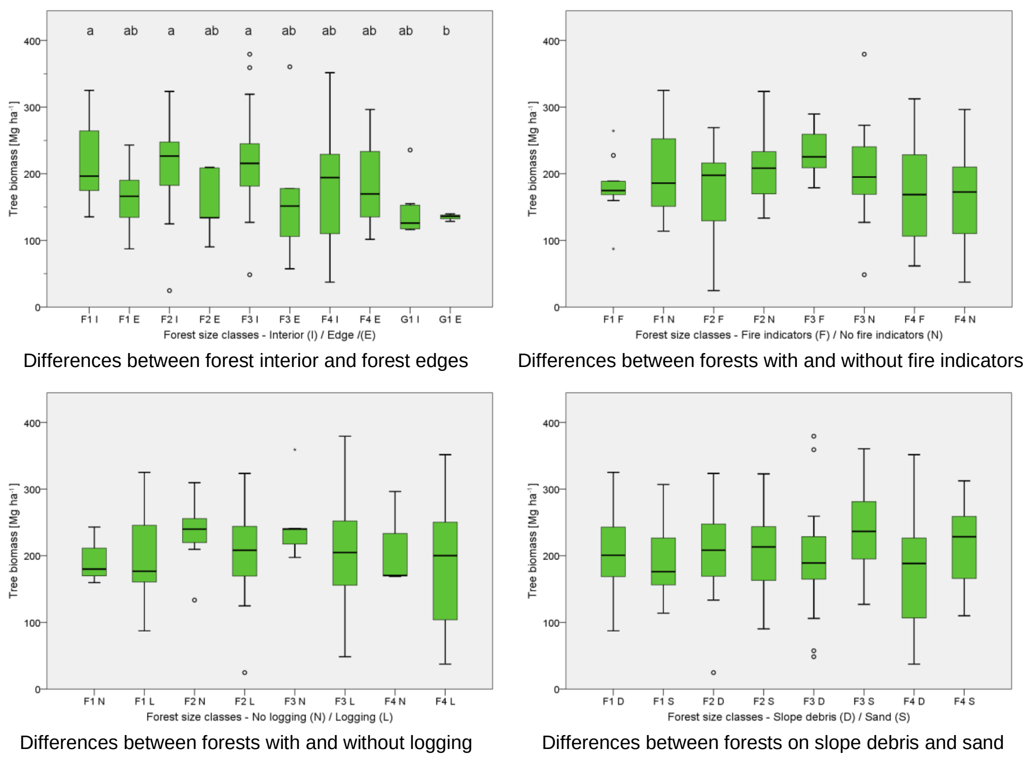

Figure 5: Boxplots of tree biomass (Mg ha^{-1}) related to different site conditions. Horizontal line = median, bars = quartiles, whiskers = range, dots = outliers. A Duncan Posthoc test (p <0.05) showed that most of the datasets were not statistically different. Significant differences existed between the forest interior and forest edges.

https://doi.org/10.5194/bg-2020-13
Preprint. Discussion started: 3 March 2020

Biogeosciences
Discussions
Open Access
EGU

4.3. Remote-sensing analyses based on tree biomass estimates

We tested several NDVI datasets, calculated from Sentinel 2 and Landsat 8 satellite images of the years 2013-2018, and various topographic parameters (see Figure 3) based on TanDEM-X data, for significant single or multi-correlations ($r > 0.5$, $p < 0.05$) with the measured tree biomass, since such correlations would allow for interpolation of tree biomass. However, we found no statistically significant correlations. The low number of cloud-free (<10 % cloud cover) multispectral satellite images of the summer seasons was one obstacle for NDVI analysis. Weak correlation between needle volume and tree biomass caused another problem, as the leaves and needles provide the vitality signal to be measured in multispectral satellite images. Danilin and Tsogt (2014) stated that needle biomass is independent of the average age of a larch stand, whereas tree biomass increases with average tree age. The weak correlation between leaf area index (LAI) and tree biomass measured on 24 plots confirmed this statement (Figure 6). Thus, the statistical relationships between NDVI, needle volume and tree biomass were poor.

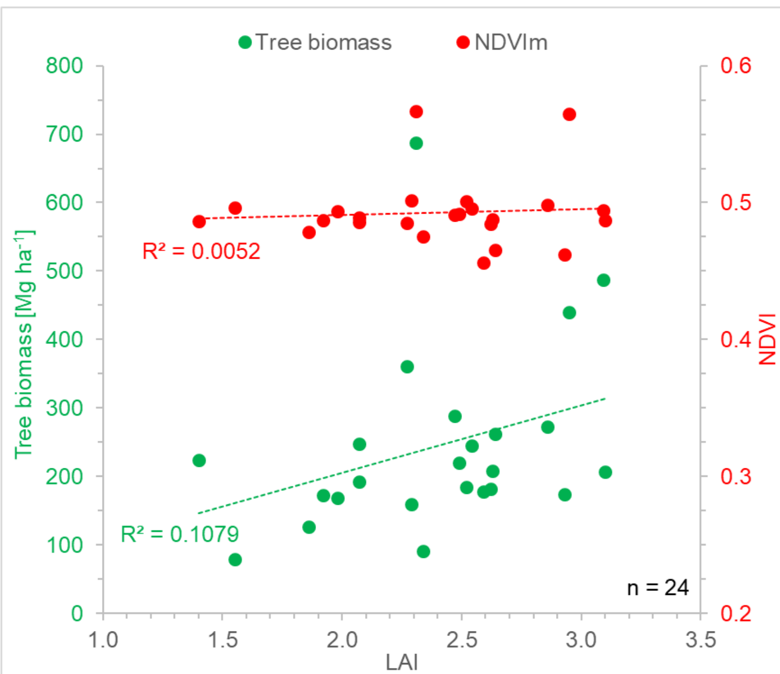

https://doi.org/10.5194/bg-2020-13
Preprint. Discussion started: 3 March 2020

Figure 6: Relationships between $NDVI_m$ (red) and leaf area index (LAI), and between tree biomass on 24 plots of the study area (green) and LAI.

The phenology of the deciduous larch trees and the ground vegetation created another problem for the NDVI signal. Various topo-climatic conditions, e.g., cold air masses cumulating in topographic depressions during spring, cool conditions at higher elevations, droughts in late summer, produce temporally and spatially inhomogeneous patterns of tree vitality and thus NDVI. Therefore, we calculated mean NDVI values ($NDVI_m$) of seven Sentinel 2 images of the growing seasons 2016-2018 to obtain more site-representative NDVI values (Figure 7). $NDVI_m$ was lower at the forest edges than in the forest interiors. It was also lower in small larch stands in steppe-dominated areas (G_1) than in small larch stands in forest-dominated areas (F_1). The high variation and the corresponding trend lines illustrate the low statistic correlation between tree biomass and $NDVI_m$ for the measuring plots (Figure 7). Due to the low canopy closure of the larch forests of less than 53 %, the NDVI represents a signal for the vegetation vitality of both the trees and the understorey, which disabled an expedient tree biomass interpolation.

https://doi.org/10.5194/bg-2020-13
Preprint. Discussion started: 3 March 2020

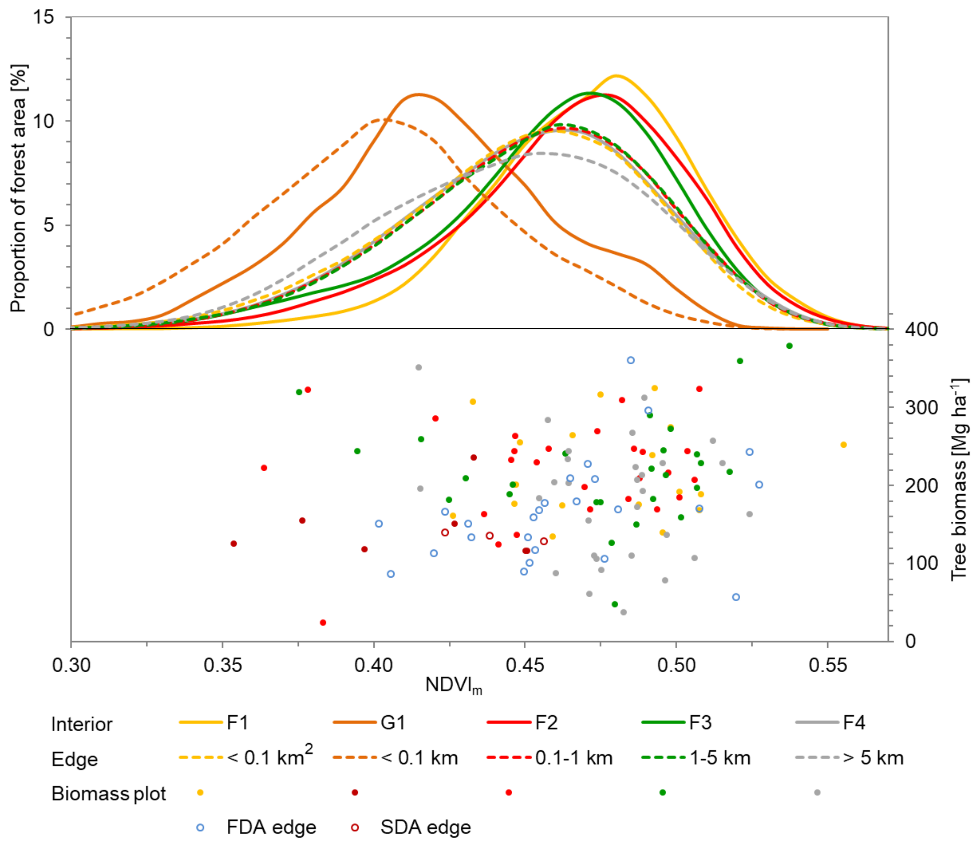

Figure 7: Top - NDVI$_m$ frequency distribution curves for the interior and edges of larch stands of the five forest-size classes. Bottom – Tree biomass plotted against NDVI$_m$.

4.4.1. PFA delineation based on relief parameters (PFA$_r$)

In 1986, the upper treeline in the southern HMA reached up to 2,600 m a.s.l. (Figure 8), and forests occurred up to a maximum inclination of 25°. Since then, forest distribution showed a shift in both altitude and aspect (Figure 8). Because of forest fires in the upper mountains, the mean elevation range of the actual forests (95 %) has been restricted to 1,600-2,400 m a.s.l. These changes coincided with a transition from mountain forest-steppe to mountain subtaiga and the occurrence of *Pinus sibirica* in the uppermost forest areas. South-facing slopes in the forest-steppe are generally covered by steppe vegetation and partially forested above 2,100 m a.s.l. (Figure 8). MGS insolation increases

https://doi.org/10.5194/bg-2020-13
Preprint. Discussion started: 3 March 2020

by approximately 90 kW h m^{-2} per 100 m elevation. The maximum MSG insolation occurring on the south-facing slopes exceeds that on the east- and west-facing slopes by ca. 50 kW h m^{-2}, and that on the north-facing slopes by 100 kW h m^{-2}. Forests also occur in areas of maximum MGS insolation (Figure 8), which demonstrates that insolation is no limiting factor for forest distribution in the study area.

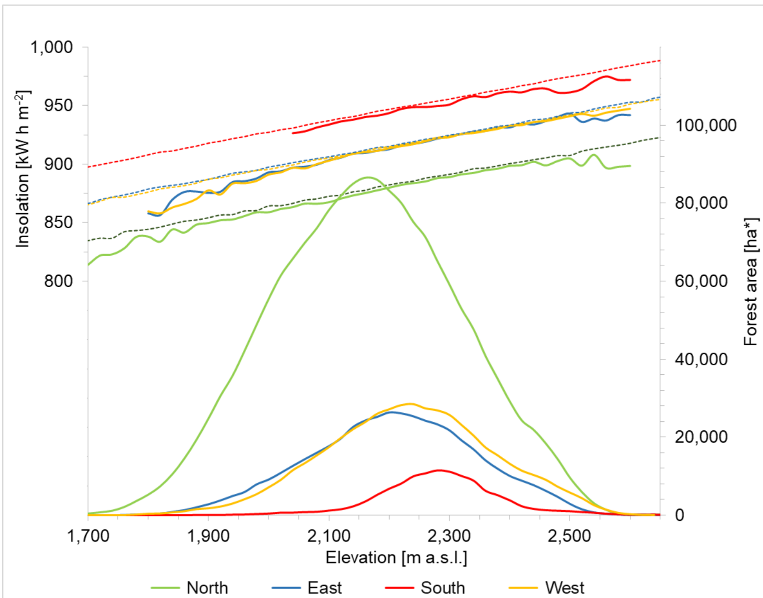

*Figure 8: Top - Change of maximum MGS insolation (left axis) with elevation (MGS = mean growing season, May-September). Solid lines = MGS insolation on forest area, dashed lines = MGS insolation on the total land surface. Bottom - Forest area in hectares (right axis) in 1986 plotted against elevation. * The forest area on south-exposed slopes is shown in ha x10.*

According to the observed relief-controlled hydrological limitations of forest distribution, we used the processed TanDEM-X data to identify the PFA$_r$ as the area, where all three parameters aspect, slope gradient and elevation allowed for tree growth (Figure 10). Thereby, we excluded forests in alluvial plains (areas with inclinations ≤2.5° along rivers and in basins), because their hydrological limitations are not controlled by the same parameters but rather by groundwater availability. The most striking outcome of this PFA$_r$ modelling was a much more extensive forest cover on toe slopes

https://doi.org/10.5194/bg-2020-13
Preprint. Discussion started: 3 March 2020

and pediments, which are at present generally covered by steppe vegetation (Figure 10). In the HMA, the modelled PFA_r exceeded the presently forested area on steep slopes, from the valleys up to the upper treeline at 2,600 m a.s.l. The PFA_r did not cover 3.4 % of the forest area that existed in 1986.

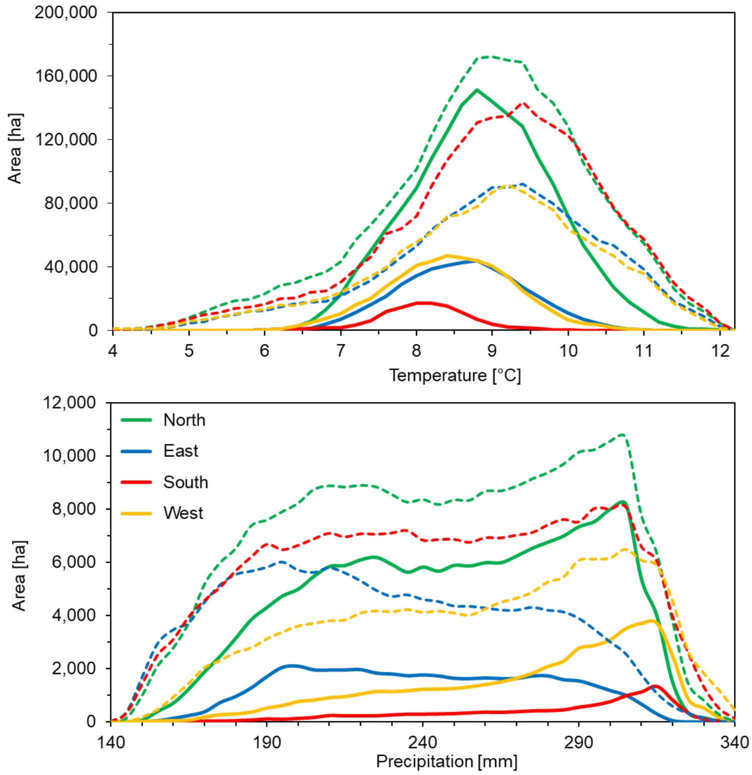

Figure 9: Frequency distribution curves of mean growing season temperature (MGST) and mean annual precipitation (MAP) in the study area. Solid lines = forest area, dashed lines = total area. Climate data source: CHELSA V1.2 (Karger et al., 2017), period 1979–2013, spatially resampled to 30 m by linear interpolation.

4.4.2. PFA delineation based on climatic parameters (PFA_c)

In a second PFA estimation approach, we analysed the forest distribution of 1986 for relationships with various climate parameters (Figure 9). Potential evaporation was so closely correlated with MGST that it appeared not necessary to include it as an additional parameter for delineating the PFA_c. The spatial resampling of the climate data by linear interpolation produced some noise in the

https://doi.org/10.5194/bg-2020-13
Preprint. Discussion started: 3 March 2020

data, because it could not consider small topographic variations. Therefore, we did not use them to deduce the threshold values for forest growth. Instead, we defined the threshold values based on the most accurate visual overlap of the PFA and the forest distribution of 1986. The resulting thresholds are listed in Table 2. The obtained PFA_c showed larger forest areas on the upper south-facing slopes and small flat summits. It matched well with the upper treeline in the HMA (Figure 10). Compared to the PFA_r, the PFA_c did not extend as far down into the basins, which may be due to the low precipitation there. The PFA_c did not cover 5.1 % of the forest area that existed in 1986.

Table 2: Climatic thresholds for PFA_c delineation based on the mean growing season temperature (MGST) and mean annual precipitation (MAP)

	Aspect			
	North	East	South	West
Maximum MGST [°C]	10.8	10.4	8.6	10.0
Minimum MGST [°C]	6.5	6.5	6.5	6.5
Maximum MAP [mm]	320	310	340	340
Minimum MAP [mm]	160	170	290	165

https://doi.org/10.5194/bg-2020-13
Preprint. Discussion started: 3 March 2020

Biogeosciences
Discussions
Open Access
EGU

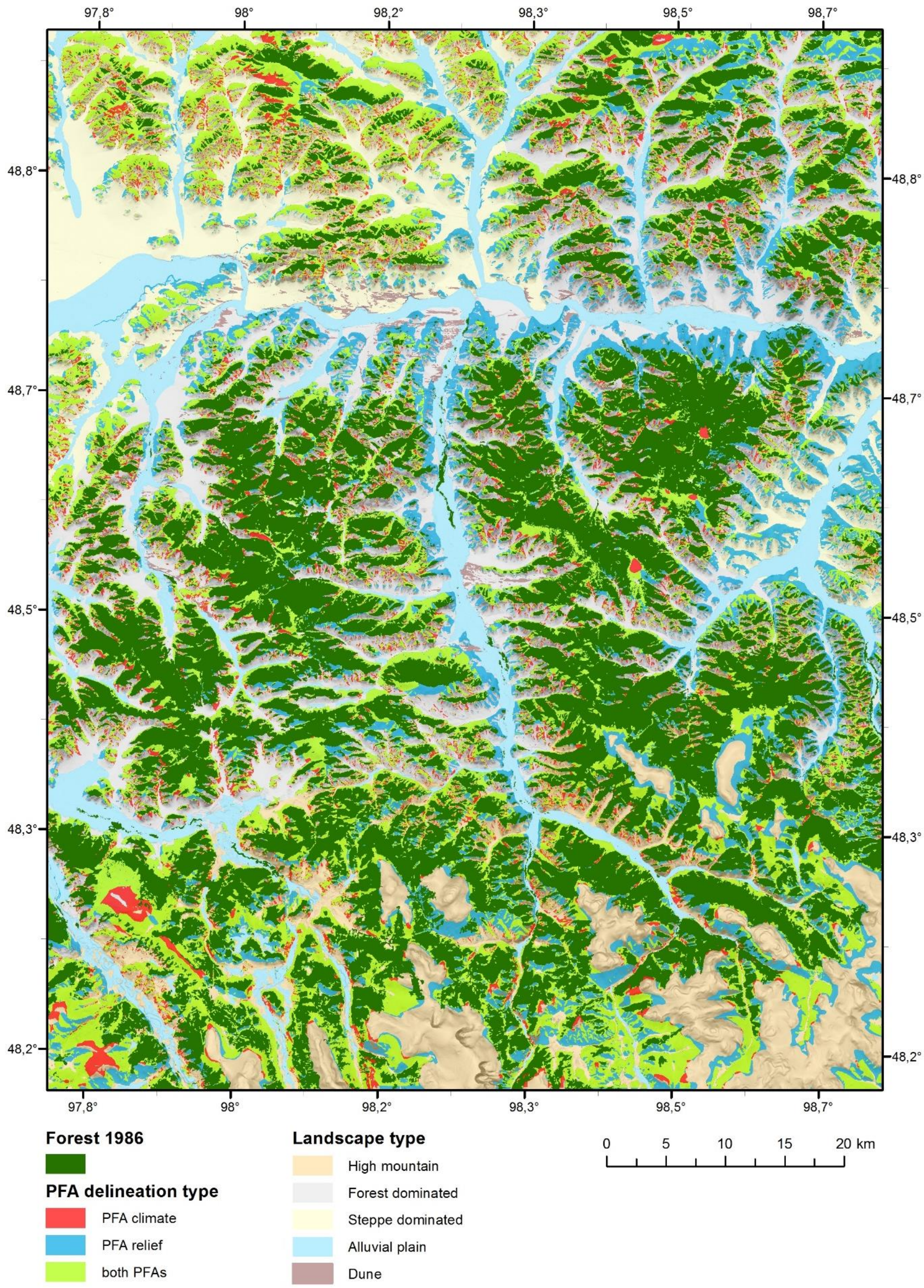

Figure 10: Forest distribution in 1986 and potential forest areas (PFA) delineated based on climate and relief. The shaded relief illustration is based on TanDEM-X data.

https://doi.org/10.5194/bg-2020-13
Preprint. Discussion started: 3 March 2020

4.5. Aggregated results of the forest area and tree biomass assessments and modelling

The size of the study area was 6,355 km^2, whereby two thirds (4,457 km^2) were originally covered by steppe vegetation. At present, the total forest area (AFA) amounts to 1,086 km^2, whereas in 1986 it was 1,898 km^2. The modelled PFA yielded 3,168 (PFA_c) and 3,553 km^2 (PFA_r), respectively. Details on the differences between the AFA, forest area in 1986, and PFA, differentiated according to forest and landscapes types, are listed in Tables 3 and 5. The largest portion of the actual forest area occurs in the forest size class (FSC) F4 (8.6 %). Prior to the large fire events, this FSC was also widespread in the HMA (9.2 %). Altogether, a forest area of 812.5 km^2 (12.8 % of the total study area and 42.8 % of the former forest area) was destroyed by fire since the end of the last century. The BFA was negligible in the SDA and small in the FDA, but it amounted up to 95 % of the former forest area in the HMA. The ratios between forest interior and forest edge (F_i/F_e) for each FSC were relatively consistent for the different landscape units. However, the F_i/F_e ratios of the AFA tended to be lower than those of the forest areas in 1986, indicating an increase in forest fragmentation (Table 3).

Table 3: Dimensions [km^2] and relative portions [%] of different forest and landscape types in the study area at present (AFA) and in 1986, prior to the large forest fires (FSC = forest size class)

https://doi.org/10.5194/bg-2020-13
Preprint. Discussion started: 3 March 2020

	Actual forest area AFA					Forest distribution in 1986				
FSC	1	2	3	4	Burned forest	1	2	3	4	Steppe
absolute area of forest landscape type [km²]										
Steppe dominated SDA										
Interior	4.74	18.25	21.51	7.29	3.88	5.59	19.65	22.90	7.92	1042.29
Edge	11.07	12.33	7.65	1.69		10.28	16.19	6.92	1.37	
Ratio I/E	0.43	1.48	2.81	4.32		0.54	1.21	3.31	5.80	
Forest dominated FDA										
Interior	12.66	82.93	144.04	440.35	115.25	13.90	87.52	120.78	606.55	1907.62
Edge	43.55	52.56	44.21	107.34		32.10	42.10	32.12	105.36	
Ratio I/E	0.29	1.58	3.26	4.10		0.43	2.08	3.76	5.76	
High mountain HMA										
Interior	1.73	7.51	6.40		693.33	3.74	29.70	65.66	491.08	1021.74
Edge	13.06	6.73	2.32			10.70	15.92	20.71	93.56	
Ratio I/E	0.13	1.12	2.76			0.35	1.87	3.17	5.25	
Alluvial forest	3.98	3.42	1.09		0.05	2.74	2.74	2.74		485.74
Dune						0.01				27.28
Relative proportion of landscape type [%]										
Steppe dominated SDA										
Interior	0.07	0.29	0.34	0.11	0.06	0.09	0.31	0.36	0.12	16.40
Edge	0.17	0.19	0.12	0.03		0.16	0.25	0.11	0.02	
Sum	0.25	0.48	0.46	0.14		0.25	0.56	0.47	0.15	
Forest dominated FDA										
Interior	0.20	1.30	2.27	6.93	1.81	0.22	1.38	1.90	9.54	30.02
Edge	0.69	0.83	0.70	1.69		0.51	0.66	0.51	1.66	
Sum	0.88	2.13	2.96	8.62		0.72	2.04	2.41	11.20	
High mountain HMA										
Interior	0.03	0.12	0.10		10.91	0.06	0.47	1.03	7.73	16.08
Edge	0.21	0.11	0.04			0.17	0.25	0.33	1.47	
Sum	0.23	0.22	0.14			0.23	0.72	1.36	9.20	
Alluvial forest	0.13				0.001	0.04	0.07	0.02		7.64
Dune										0.43

Due to the low correlation between NDVI and tree biomass (Figures 6 and 7), estimation of the total tree biomass of the study area by use of regression functions was not feasible. Thus, we estimated the total tree biomass by multiplying the specific mean tree biomass of each forest type (Table 1) with the corresponding area of the respective forest type (Tables 3 and 5). The mean tree biomass for the HMA was adapted from the FDA. As the modelled PFAs resulted in forest-dominated landscapes, we used the FDA tree-biomass mean values for estimating the total tree biomass in the study area corresponding to the PFA (Table 5). The actual tree biomass in the study area is 57 % of the one in 1986, corresponding to 30 % and 34 % of the tree biomass estimated for the PFA_r and PFA_c, respectively (Table 5). The greatest losses of tree biomass due to forest fires were detected in the large forests (size class F4) of the FDA and HMA, whereas the tree biomass losses due to fire were less severe in the SDA and alluvial forests.

https://doi.org/10.5194/bg-2020-13
Preprint. Discussion started: 3 March 2020

Table 4: Total tree biomass [10^6 g] in the different forest types of the study area

Actual forest area AFA						Forest distribution in 1986				
FSC	1	2	3	4	Sum	1	2	3	4	Sum
Steppe dominated SDA										
Interior	68,892	398,195	474,487	132,398	1,073,972	81,348	428,835	505,209	143,948	1,159,341
Edge	149,217	191,236	130,499	31,053	502,005	138,668	251,237	118,171	25,152	533,229
Sum	218,109	589,431	604,986	163,450	1,575,976	220,016	680,073	623,380	169,100	1,692,569
Forest dominated FDA										
Interior	277,732	1,809,560	3,177,481	8,000,534	13,265,306	304,883	1,909,714	2,664,408	11,020,218	15,899,224
Edge	718,971	815,498	754,423	1,977,866	4,266,758	530,041	653,229	548,092	1,941,327	3,672,689
Sum	996,703	2,625,058	3,931,904	9,978,400	17,532,064	834,925	2,562,943	3,212,500	12,961,545	19,571,913
High mountain HMA										
Interior	37,963	163,881	141,084	0	342,928	82,118	648,002	1,448,389	8,922,284	11,100,793
Edge	215,657	104,498	39,519	0	359,674	176,719	247,038	353,449	1,723,920	2,501,126
Sum	253,620	268,379	180,603	0	702,602	258,837	895,041	1,801,838	10,646,204	13,601,919
Alluvial forest	350,149					353,095				
Total Sum					20,160,791					35,219,497
Comparison of tree biomasses										
Sum 1986	1,313,778	4,138,056	5,637,718	23,776,849	34,866,401					
Sum 2018	1,468,432	3,482,868	4,717,493	10,141,850	19,810,642					
Loss by fire	-154,655	655,189	920,225	13,634,999	15,055,759					
%	-11.8	15.8	16.3	57.3	43.2					

Table 5: Potential forest area (PFA) and tree biomass as influenced by climate and relief

	Potential forest area PFA climate					Potential forest area PFA relief				
FSC	1	2	3	4	Steppe area	1	2	3	4	Steppe area
Area [km^2]										
Interior	11.49	69.21	77.30	2590.66	2692.99	11.17	69.52	91.04	2940.99	2308.48
Edge	35.06	38.45	23.15	322.99		38.46	42.14	28.87	330.62	
Ratio I/E	0.33	1.80	3.34	8.02		0.29	1.65	3.15	8.90	
Tree biomass [x10^6 g]					Total sum					Total sum
Interior	251,930	1,510,158	1,705,159	47,068,688	50,535,934	245,059	1,516,857	2,008,287	53,433,781	57,203,985
Edge	578,839	596,605	395,092	5,951,310	7,521,845	635,056	653,769	492,614	6,091,966	7,873,404
Sum	830,768	2,106,762	2,100,250	53,019,998	58,057,779	880,115	2,170,625	2,500,901	59,525,748	65,077,389
Comparison of tree biomasses [x10^6 g]										
PFA - 1986	-483,009	-2,031,294	-3,537,468	29,243,149	23,191,377	-433,662	-1,967,431	-3,136,817	35,748,898	30,210,988
%	-58.1	-96.4	-168.4	55.2	39.9	-49.3	-90.6	-125.4	60.1	46.4
PFA - 2018	-637,664	-1,376,105	-2,617,242	42,878,148	38,247,136	-588,317	-1,312,242	-2,216,592	49,383,898	45,266,747
%	-76.8	-65.3	-124.6	80.9	65.9	-66.8	-60.5	-88.6	83.0	69.6

5. Discussion

This study showed that the Mongolian forest steppe is characterised by highly variable tree biomass. The differences in mean tree biomass between various forest types were up to 85 Mg ha^{-1}. In addition to natural impacts on forests (e.g., fire, windbreak, insect calamities, and drought), logging and forest pasture strongly affect forest distribution and tree biomass. Large alluvial forests exist where river channels hamper wood pasture, logging, and forest fires. These alluvial forests usually consist of old larch trees with large tree biomass. Larch trees on dunes are also very old, but they occur isolated and have a low stand density.

https://doi.org/10.5194/bg-2020-13
Preprint. Discussion started: 3 March 2020

The main natural factors that control the vitality and spatial distribution of forests in the Mongolian forest-steppe are limited precipitation and high evapotranspiration. The latter depends on insolation, which in turn varies with topography. These factors cause the lack of forests on south-facing slopes (Klinge et al., 2018; Hais et al., 2016; Dulamsuren and Hauck, 2008).

The forest canopy supports dense ground vegetation and an organic surface layer that insulates the soil and serves as moisture reservoir during summer (Dashtseren et al., 2014). In this way, forests facilitate discontinuous permafrost. In turn, in this semi-arid region, the presence of permafrost plays an important role for tree survival during summer droughts, as it provides meltwater throughout the summer (Sugimoto et al., 2002). Recognising these mutual relationships between tree density, forest canopy closure, ground vegetation, organic surface layer, and the occurrence of permafrost is crucial for understanding the patterns of forest distribution and tree biomass.

Our tree biomass measurements in the field showed that the least mean tree biomasses occurred in the forest size class G1 (142 Mg ha^{-1}) of the SDA and in the class F4 (182 Mg ha^{-1}) of the FDA. The fragmented forests in the SDA generally have lower tree densities and thus provide less shade. As a result, there is no permafrost under these forests, and the majority of the ground vegetation consists of grasses with a species composition similar to that of the surrounding steppes. Forests of the FDA have higher tree densities and support a dense ground vegetation cover consisting of herbs, shrubs, grasses and mosses, and an organic surface layer, which together enable the development of permafrost through its insulation effect (Dashtseren et al., 2014).

Forest edges represent natural zones of forest expansion and retreat (Sommer and Treter, 1999). Temporally varying climate conditions control the position and shifts of the forest edges. Thus, the forest edges may have a fringe of dead trees at their outer boundary, and their outer boundaries may also be dissected. In addition, logging and pasture is more intensive at the forest edges than in the interiors. Due to the lower tree density, the tree biomasses are generally lower at the forest edges than in the interiors. However, we found exceptions to this role in the forest size classes G1 and F4, where the forest interiors and edges had similar tree biomasses. In the class G1, the tree biomasses of the small interior forest areas are similarly low as those of the forest edges. In the class

F4, the forest edges have large tree biomasses compared to all other forest edges. However, the tree biomass in the interior of these large forest stands is not much greater, because permafrost that already occurs at shallow depth hinders the trees from deep rooting. Hence, the trees can reach less nutrient stocks and are prone to windthrow. Thus, permafrost plays a twofold role in these large forests. On the one hand, it causes the low mean tree biomass in the forest interior. On the other hand, it enhances the vitality of trees at the forest edges through meltwater supply during summer. This effect, together with higher precipitation in the upper mountains may also explain the existence of forests on south-facing slopes in the higher mountains (Figure 8).

The forest area that burnt down between 1986 and 2017 (BFA) amounts to 12.8 % of the total study area. The loss of tree biomass since the last century adds up to roughly 15 million t, which represents more than 45 % of the former tree biomass. Although the most extensive forest fires in this area occurred already in 2002, forests have not yet re-established in many parts of the BFA. The most extensive BFAs are located in the large continuous forests of the HMA and in the upper parts of the mountains in the FDA. In contrast, only few BFAs occur in the small and fragmented forests of the SDA. We thus conclude that forest fragmentation in the SDA prevents forest fires from passing over into neighbouring forest stands and keeps fires more isolated. The decrease of large forests (size class F4) by fire led to an increase in small-sized fragmented forest stands (size class F1) of surviving trees, representing remnants of the former large forests. This change induced the loss of permafrost in these areas. The surviving larch trees in the remaining forest remnants increase their fructification (Danilin and Tsogt, 2014). Their important role as nuclei for forest regeneration is demonstrated by numerous seedlings and saplings growing in the direct surrounding of the forest remnants, in the shade of the old trees. Thus, a slow but steady re-immigration of larch trees into the burned area proceeds from these forest remnants. It takes up to 200 years until a forest regenerates to its previous state before the fire (Nyamjav et al., 2007).

Fires occur frequently in semi-arid environment (Hessl et al., 2012). Thus, *Larix sibirica* is to a certain degree fire-adapted. Its survival of a fire depends on the type of fire (crown, surface or ground fire),

https://doi.org/10.5194/bg-2020-13
Preprint. Discussion started: 3 March 2020

fire intensity, season and soil moisture. The prevalent survival of forest stands in depressions, erosion channels, and on toe slopes demonstrates the importance of soil moisture for tree survival.

Forest stands that experienced non-lethal fire events or selective logging have similar tree biomasses as pristine forests. We conclude that moderate thinning of forests may improve the growing conditions for the remaining trees, possibly because of less competition by other trees and additional nutrient supply from ash, and because the melting permafrost leads to a temporary increase of soil moisture and allows for deeper rooting.

The delineation of the PFA_r (based on relief) suggests a potential for forest expansion, both down towards the basins and up the mountains. The pediments generally provide suitable geoecological conditions for tree growth, as confirmed by several small forest stands. Nevertheless, steppe vegetation predominates on the pediments, mainly because of herbivore grazing (Hilbig, 1995). The lower treeline of the PFA_c (based on climate), considering the restriction of tree growth by dry conditions in the basins, coincides with that of the actual forest. Existence of forests below the threshold of 160 mm MAP can be explained by site-specific additional water influx. The PFA_c moreover suggests a potential for more forests on south-facing slopes. This mismatch indicates that MAP and MGST alone cannot explain forest distribution, which is apparently a result of more complex causal chains, involving relief, climate, geo- and bioecological factors and mutual interactions between them.

Cool conditions restrict the expansion of forests into upper valleys and onto the mountain plateaus of the HMA in the South. Short growing seasons and long-lasting snow cover prevent tree growth there. Another limiting factor is the extensive use of the alpine meadows as summer pastures by nomads for a long time. The upper treeline varies from 2,200 m a.s.l. in the north of the study area to 2,550 m a.s.l. in the south. Thereby, the small treeless areas on the flat peaks of the northern mountains may result from the so-called “summit effect” (Körner, 2012), i.e., particularly harsh conditions near summits, rather than from a true upper treeline.

The modelled PFAs show large forest stands in the SDA in the north. These would turn that area into FDA. The number of small fragmented forest stands would strongly decrease. Thus, given the

https://doi.org/10.5194/bg-2020-13
Preprint. Discussion started: 3 March 2020

permafrost-promoting effect of large forests, also permafrost distribution would considerably increase in that area. This points to the possibility that the forest area in the SDA might have been reduced by logging.

The modelled maximum tree biomass of the PFA (58-65 $x10^9$ g) was twice the tree biomass of 35 $x10^9$ g in 1986 and three times the actual tree biomass of 20 $x10^9$ g. However, several relevant factors could not be considered in the PFA modelling. For example, large forests (size class F4), as predominantly obtained from the PFA modelling, are more likely exposed to severe fires than fragmented forest stands. In addition, due to the long-lasting human influence, the natural proportion between steppe and forest in this region remains a major research challenge (Klinge and Sauer, 2019). Human impact already started with the extinction of large herbivores like elephantine, and the reduction of wild animal herds since the Mesolithic period. It continued with the breeding of domestic animals and the development of pasture economy since the Neolithic period.

Tchebakova et al. (2009) modelled potential vegetation changes across Siberia based on climate change scenarios projecting warmer and drier climate. The authors reported an increase of forest-steppe and grassland areas. More frequent and severe wildfires would occur stimulated by dry conditions and enhanced by more fire load due to increased tree mortality. Nyamjav et al. (2007) stated that 95% of the actual forest destruction was caused by forest fires, whereas 5% was referred to logging. The authors reported an increase of fire events in Mongolia during the past decades and Goldammer (2002) assumed that most of the fires were caused by human activities. Hessl et al. (2012) investigated fire history since the last 450 years based on tree ring analysis. Concordant with results from the Tuva region in southern Siberia (Ivanova et al., 2010), the authors did not find a distinct increase of fire frequency during the last decades but fire events became more severe due to drier conditions. The limited synchrony of fire events between different sites points to human caused ignitions (Hessl et al., 2012). Human impact on biomass reduction, due to fuel wood gathering and intensive grazing of livestock may reduce available fuel for fire, which makes them less severe and extensive (Hessl et al., 2012; Umbanhowar et al., 2009).

https://doi.org/10.5194/bg-2020-13
Preprint. Discussion started: 3 March 2020

6. Conclusions

A combination of tree biomass and soil mapping, remote sensing and climate data analysis allowed us to identify factors affecting larch forest distribution and tree biomass in the northern Khangai Mountains, central Mongolia, and to model the potential larch forest distribution and tree biomass. Forest distribution is strongly influenced by the relief-controlled climatic key factors precipitation, evapotranspiration, temperature, soil moisture, and presence of permafrost. Forests of different types and landscape units have similar tree biomass. Only forest edges and small fragmented forest stands have less tree biomass than all other units. None-lethal fires have no serious impact on tree biomass. Selective logging involves removal of tree biomass, but it also stimulates tree growth by moderately reducing the tree density and thus competition. The NDVI is not suitable for estimating tree biomass in the forest-steppe.

Forest fires destroyed 43 % of the forest area and 45 % of the tree biomass in the study area over the period 1986-2017. They mostly affected large forest stands (size class F4) in the upper mountains of the FDA and HMA. Fragmented forests of the SDA are less prone to severe fires because of their spatial isolation. Forest fires increase the number of small forest stands (size class F1), because often small remnants of the formerly large forests survive at sites with increased soil moisture (e.g., depressions, toe slopes). Permafrost, which is widespread under large forests, disappears soon after the destruction of a large forest stand (F4).

The factors aspect, slope gradient and elevation, and high-resolution precipitation and temperature data are suitable parameters for modelling the PFA. We obtained a PFA_r of 3,552 km^2 with 65 $x10^9$ g tree biomass, based on relief parameters, and a PFA_c of 3,113 km^2 with 58 $x10^9$ g tree biomass, based on climatic parameters, corresponding to more than 288 % and 323 % of the actual tree biomass, respectively. However, these approximations do not yet consider several relevant factors such as herbivore grazing and plant competition. In addition, human impact plays an important role, which is difficult to quantify.

7. Acknowledgements

We thank Ms. Daramragchaa Tuya from the Tarvagatai Nuruu National Park (Tosontsengel Sum, Zavkhan Aimag, Mongolia) for her invaluable support of our research. We wish to express our gratitude to our Mongolian colleagues Mr. Amarbayasgalan, Mr. Enkhjargal, Mr. Enkh-Agar, Ms. Munkhtuya. We greatly appreciated their hospitality and help with the fieldwork. Our thanks also go to the German students Martine Koob, Tino Peplau, Janin Klaassen and Tim Rollwage for their great support with the biomass measurements during the fieldwork in Mongolia.

The German Aerospace Centre (DLR) liberally provided the TanDEM-X data for the study area (DEM_FOREST 1106). The fieldwork in 2014 was funded by the Volkswagen Foundation in the frame of the project 87175 "Forest regeneration and biodiversity at the forest-steppe border of the Altay and Khangay Mountains under contrasting development of livestock numbers in Kazakhstan and Mongolia". The subsequent work was funded by the Deutsche Forschungsgemeinschaft (DFG), project number 385460422.

https://doi.org/10.5194/bg-2020-13
Preprint. Discussion started: 3 March 2020

Biogeosciences Discussions
Open Access

Appendix

Table A1: Mean tree biomass (above and belowground) for different forest types and site conditions. Plots, where site conditions were not clearly identified, were excluded from the respective part of the analysis. The two lower and higher forest size classes (FSC) in the forest-dominated area (FDA) were combined for the statistical analysis, because of the small dataset for forest edges. SE = standard error, n = number of plots. Underlined data are not representative because of insufficient size of the respective dataset.

	F1	SE	*n*	F2	SE	*n*	F3	SE	*n*	F4	SE	*n*	G1	SE	*n*
total	**198.7**	11.2	*29*	**208.0**	11.8	*31*	**212.5**	13.9	*31*	**182.0**	12.9	*34*	**142.2**	10.7	*10*
difference interior - edge	**54.2**			**63.0**			**49.9**			**-2.6**			**10.6**		
forest interior	219.3	14.0	*18*	218.2	12.6	*26*	220.6	13.4	*26*	181.7	13.8	*30*	145.4	15.0	*7*
no fire indicators;															
no wood harvest			*0*	236.9	4.4	*3*	232.8	6.3	*3*	161.1	13.1	*13*			
no fire indicators	242.0	27.2	*7*	212.0	13.5	*12*	201.7	17.3	*16*	165.1	13.5	*20*	122.1	2.7	*2*
fire indicators	194.4	15.9	*5*	181.9	25.8	*8*	231.3	14.4	*6*	177.2	49.5	*4*	154.9		*1*
difference	**47.6**			**30.1**			**-29.6**			**-12.0**					
no wood harvest				255.2	10.9	*6*	251.0	25.2	*5*	174.1	14.4	*15*			
wood harvest	219.3	14.0	*18*	207.1	15.2	*20*	215.1	15.6	*20*	189.3	23.5	*15*	145.4	15.0	*7*
difference				**48.1**			**35.9**			**-15.2**					
slope debris	236.5	25.4	*7*	216.2	18.8	*15*	215.8	19.8	*15*	175.2	15.0	*25*			
sand layer	208.4	15.2	*11*	220.9	15.2	*11*	227.2	16.3	*11*	214.1	31.7	*5*			
difference	**28.1**			**-4.7**			**-11.4**			**-38.9**					
forest edge	165.1	13.7	*11*	155.2	21.0	*5*	170.7	46.2	*5*	184.3	35.2	*4*	134.8	2.7	*3*
no fire indicators;															
no wood harvest	211.5	22.3	*2*	171.5	26.9	*2*	177.8		*1*	233.4	44.6	*2*			
no fire indicators	167.5	16.0	*7*	171.5	26.9	*2*	170.7	46.2	*5*	189.4	46.6	*3*			
fire indicators	160.9	24.9	*4*	144.3	28.3	*3*				168.7		*1*			
difference	**6.6**			**27.2**						**20.7**					
no wood harvest	211.5	22.3	*2*	171.5	26.9	*2*	177.8		*1*	211.8	34.5	*3*	134.1	4.0	*2*
wood harvest	154.8	13.8	*9*	144.3	28.3	*3*	168.9	57.8	*4*	101.6		*1*	136.3		*1*
difference	56.7			27.2			9.0			110.3					
slope debris	181.2	20.9	*6*	171.5	26.9	*2*	123.2	22.9	*4*	189.4	46.6	3			
sand layer	145.8	11.7	*5*	144.3	28.3	*3*	360.5		*1*	168.7		1			
difference	**35.5**			27.2			-237.3			20.7					

combined classes	F1 / F2	SE	*n*	F2 / F3	SE	*n*	F3 / F4	SE	*n*
forest edge	162.0	11.5	*16*	162.9	25.5	*10*	176.7	30.2	*9*
no fire indicators;									
no wood harvest	191.5	20.1	*4*	173.6	18.0	*3*	214.9	33.3	*3*
no fire indicators	168.4	13.8	*9*	170.9	33.9	*7*	177.7	33.9	*8*
fire indicators	153.8	18.9	*7*	144.3	28.3	*3*	168.7		*1*
difference	**14.6**			**26.6**			9.0		
no wood harvest	191.5	20.1	*4*	173.6	18.0	*3*	203.3	26.9	*4*
wood harvest	152.2	12.6	*12*	158.3	35.5	*7*	155.4	33.3	*3*
difference	**39.3**			**15.3**			**47.9**		
slope debris	169.9	14.9	*10*	139.3	20.0	*6*	151.6	26.9	*7*
sand layer	144.2	11.5	*9*	198.3	51.4	*4*	264.6	67.8	*2*
difference	**25.7**			**-59.0**			- 113.0		

Biogeosciences Discussions
Open Access

References

Academy of Sciences of Mongolia and Academy of Sciences of USSR: National Atlas of the Peoples Republic of Mongolia, Ulan Baatar, Moscow, 144 pp., 1990.

Batima, P., Natsagdorj, L., Gombluudev, P., and Erdenetsetseg, B.: Observed climate change in Mongolia, AIACC Working Papers, 12, 1–25, 2005.

Battulga, P., Tsogtbaatar, J., Dulamsuren, C., and Hauck, M.: Equations for estimating the above-ground biomass of Larix sibirica in the forest-steppe of Mongolia, J. Forestry. Res., 24, 431–437, doi:10.1007/s11676-013-0375-4, 2013.

Buermann, W., Parida, B., Jung, M., MacDonald, G. M., Tucker, C. J., and Reichstein, M.: Recent shift in Eurasian boreal forest greening response may be associated with warmer and drier summers, Geophys. Res. Lett., 41, 1995–2002, doi:10.1002/2014GL059450, 2014.

Danilin, I. M. and Tsogt, Z.: Dynamics of structure and biological productivity of post-fire larch forests in the Northern Mongolia, Contemp. Probl. Ecol., 7, 158–169, doi:10.1134/S1995425514020036, 2014.

Dashtseren, A., Ishikawa, M., Iijima, Y., and Jambaljav, Y.: Temperature Regimes of the Active Layer and Seasonally Frozen Ground under a Forest-Steppe Mosaic, Mongolia, Permafrost and Periglac. Process., 25, 295–306, doi:10.1002/ppp.1824, 2014.

Deluca, T. H. and Boisvenue, C.: Boreal forest soil carbon: distribution, function and modelling, Forestry, 85, 161–184, doi:10.1093/forestry/cps003, 2012.

Dulamsuren, C. and Hauck, M.: Spatial and seasonal variation of climate on steppe slopes of the northern Mongolian mountain taiga, Grassl. Sci., 54, 217–230, doi:10.1111/j.1744-697X.2008.00128.x, 2008.

Dulamsuren, C., Hauck, M., Bader, M., Osokhjargal, D., Oyungerel, S., Nyambayar, S., Runge, M., and Leuschner, C.: Water relations and photosynthetic performance in Larix sibirica growing in the forest-steppe ecotone of northern Mongolia, Tree physiology, 29, 99–110, doi:10.1093/treephys/tpn008, 2009.

Dulamsuren, C., Hauck, M., Khishigjargal, M., Leuschner, H. H., and Leuschner, C.: Diverging climate trends in Mongolian taiga forests influence growth and regeneration of Larix sibirica, Oecologia, 163, 1091–1102, doi:10.1007/s00442-010-1689-y, 2010a.

Dulamsuren, C., Hauck, M., and Leuschner, C.: Recent drought stress leads to growth reductions in Larix sibirica in the western Khentey, Mongolia, Glob. Change Biol., 16, 3024–3035, doi:10.1111/j.1365-2486.2009.02147.x, 2010b.

Dulamsuren, C., Hauck, M., Leuschner, H. H., and Leuschner, C.: Gypsy moth-induced growth decline of Larix sibirica in a forest-steppe ecotone, Dendrochronologia, 28, 207–213, doi:10.1016/j.dendro.2009.05.007, 2010c.

Dulamsuren, C., Hauck, M., and Mühlenberg, M.: Insect and small mammal herbivores limit tree establishment in northern Mongolian steppe, Plant. Ecol., 195, 143–156, doi:10.1007/s11258-007-9311-z, 2008.

Dulamsuren, C., Khishigjargal, M., Leuschner, C., and Hauck, M.: Response of tree-ring width to climate warming and selective logging in larch forests of the Mongolian Altai, J. Plant. Ecol., 7, 24–38, doi:10.1093/jpe/rtt019, 2014.

Dulamsuren, C., Klinge, M., Bat-Enerel, B., Ariunbaatar, T., and Tuya, D.: Effects of forest fragmentation on organic carbon pool densities in the Mongolian forest-steppe, Forest Ecol. Manag., 433, 780–788, doi:10.1016/j.foreco.2018.10.054, 2019.

Dulamsuren, C., Klinge, M., Degener, J., Khishigjargal, M., Chenlemuge, T., Bat-Enerel, B., Yeruult, Y., Saindovdon, D., Ganbaatar, K., Tsogtbaatar, J., Leuschner, C., and Hauck, M.: Carbon pool densities and a first estimate of the total carbon pool in the Mongolian forest-steppe, Glob. Change Biol., 22, 830–844, doi:10.1111/gcb.13127, 2016.

Feldmann, E., Glatthorn, J., Hauck, M., and Leuschner, C.: A novel empirical approach for determining the extension of forest development stages in temperate old-growth forests, Eur. J. Forest Res., 137, 321–335, doi:10.1007/s10342-018-1105-4, 2018.

Goldammer, G.J.: Fire Situation in Mongolia, in: International Forest Fire News, 26, 75–83, 2002.

Goldammer, G.J. (Ed.): International Forest Fire News, 36, 97 pp., 2007.

Goodale, C. L., Apps, M. J., Birdsey, R. A., Field, C. B., Heath, L. S., Houghton, R. A., Jenkins, J. C., Kohlmaier, G. H., Kurz, W., Liu, S., Nabuurs, G.-J., Nilsson, S., and Shvidenko, A. Z.: Forest carbon sinks in the northern hemisphere, Ecol. Appl., 12, 891–899, doi:10.1890/1051-0761(2002)012[0891:FCSITN]2.0.CO;2, 2002.

Hais, M., Chytrý, M., and Horsák, M.: Exposure-related forest-steppe: A diverse landscape type determined by topography and climate, J. Arid Environ., 135, 75–84, doi:10.1016/j.jaridenv.2016.08.011, 2016.

Hansen, M. C., Potapov, P. V., Moore, R., Hancher, M., Turubanova, S. A., Tyukavina, A., Thau, D., Stehman, S. V., Goetz, S. J., Loveland, T. R., Kommareddy, A., Egorov, A., Chini, L., Justice, C. O., and Townshend, J. R. G.: High-resolution global maps of 21st-century forest cover change, Science (New York, N.Y.), 342, 850–853, doi:10.1126/science.1244693, 2013.

Hauck, M., Leuschner, C., and Homeier, J.: Klimawandel und Vegetation – Eine globale Übersicht, in press, Spektrum, Springer, Berlin, Heidelberg, 2019.

Hessl, A. E., Ariya, U., Brown, P., Byambasuren, O., Green, T., Jacoby, G., Sutherland, E. K., Nachin, B., Maxwell, R. S., Pederson, N., Grandpré, L. de, Saladyga, T., and Tardif, J. C.: Reconstructing fire history in central Mongolia from tree-rings, Int. J. Wildland Fire, 21, 86, doi:10.1071/WF10108, 2012.

Hilbig, W.: The vegetation of Mongolia, SPB Acad. Publ., Amsterdam, 258 pp., 1995.

IPCC: Climate Change 2013 - The Physical Science Basis, Cambridge University Press, Cambridge, 2013.

Ivanova, G. A., Ivanov, V. A., Kukavskaya, E. A., and Soja, A. J.: The frequency of forest fires in Scots pine stands of Tuva, Russia, Environ. Res. Lett., 5, 15002, doi:10.1088/1748-9326/5/1/015002, 2010.

Jacob, M., Bade, C., Calvete, H., Dittrich, S., Leuschner, C., and Hauck, M.: Significance of Over-Mature and Decaying Trees for Carbon Stocks in a Central European Natural Spruce Forest, Ecosystems, 16, 336–346, doi:10.1007/s10021-012-9617-0, 2013.

Jarvis, P., Saugier, B., and Schulze, E.-D.: Productivity of boreal forests, in: Terrestrial global productivity, Roy, J., Saugier, B., Mooney, H. (Eds.), Academic Press, San Diego, 211–244, 2001.

Karger, D. N., Conrad, O., Böhner, J., Kawohl, T., Kreft, H., Soria-Auza, R. W., Zimmermann, N. E., Linder, H. P., and Kessler, M.: Climatologies at high resolution for the earth's land surface areas, Scientific data, 4, 170122, doi:10.1038/sdata.2017.122, 2017.

Karger, D. N., Conrad, O., Böhner, J., Kawohl, T., Kreft, H., Soria-Auza, R. W., Zimmermann, N. E., Linder, H. P., and Kessler, M.: Data from: Climatologies at high resolution for the earth's land surface areas, Dryad, Dataset, https://doi.org/10.5061/dryad.kd1d4, 2018.

Karnieli, A., Bayarjargal, Y., Bayasgalan, M., Mandakh, B., Dugarjav, C., Burgheimer, J., Khudulmur, S., Bazha, S. N., and Gunin, P. D.: Do vegetation indices provide a reliable indication of vegetation

https://doi.org/10.5194/bg-2020-13
Preprint. Discussion started: 3 March 2020

degradation?: A case study in the Mongolian pastures, Int. J. Remote Sens., 34, 6243–6262, doi:10.1080/01431161.2013.793865, 2013.

Khansaritoreh, E., Dulamsuren, C., Klinge, M., Ariunbaatar, T., Bat-Enerel, B., Batsaikhan, G., Ganbaatar, K., Saindovdon, D., Yeruult, Y., Tsogtbaatar, J., Tuya, D., Leuschner, C., and Hauck, M.: Higher climate warming sensitivity of Siberian larch in small than large forest islands in the fragmented Mongolian forest steppe, Glob. Change Biol., doi:10.1111/gcb.13750, 2017.

Klinge, M., Böhner, J., and Erasmi, S.: Modeling forest lines and forest distribution patterns with remote-sensing data in a mountainous region of semiarid central Asia, Biogeosciences, 12, 2893–2905, doi:10.5194/bg-12-2893-2015, 2015.

Klinge, M., Dulamsuren, C., Erasmi, S., Karger, D. N., and Hauck, M.: Climate effects on vegetation vitality at the treeline of boreal forests of Mongolia, Biogeosciences, 15, 1319–1333, doi:10.5194/bg-15-1319-2018, 2018.

Klinge, M. and Sauer, D.: Spatial pattern of Late Glacial and Holocene climatic and environmental development in Western Mongolia - A critical review and synthesis, Quaternary Sci. Rev., 210, 26–50, doi:10.1016/j.quascirev.2019.02.020, 2019.

Körner, C.: Alpine treelines: Functional ecology of the global high elevation tree limits, Springer, Basel [u.a.], 220 pp., 2012.

Kowalkowski, K. and Starkel, L.: Altitudinal belts of geomorphic pro¬cesses in the southern Changai Mts. (Mongolia), Studia Geomorphologica Carpatho-Balcanica, 18, 95–115, 1984.

Liu, H., Park Williams, A., Allen, C. D., Guo, D., Wu, X., Anenkhonov, O. A., Liang, E., Sandanov, D. V., Yin, Y., Qi, Z., and Badmaeva, N. K.: Rapid warming accelerates tree growth decline in semi-arid forests of Inner Asia, Glob. Change Biol., 19, 2500–2510, doi:10.1111/gcb.12217, 2013.

Lu, D., Chen, Q., Wang, G., Liu, L., Li, G., and Moran, E.: A survey of remote sensing-based aboveground biomass estimation methods in forest ecosystems, Int. J. Digit. Earth, 9, 63–105, doi:10.1080/17538947.2014.990526, 2015.

Luyssaert, S., Inglima, I., Jung, M., Richardson, A. D., Reichstein, M., Papale, D., Piao, S., Schulze, E.-D., WINGATE, L., and others: CO_2 balance of boreal, temperate, and tropical forests derived from a global database, Glob. Change Biol., 13, 2509–2537, doi:10.1111/j.1365-2486.2007.01439.x, 2007.

Miao, L., Liu, Q., Fraser, R., He, B., and Cui, X.: Shifts in vegetation growth in response to multiple factors on the Mongolian Plateau from 1982 to 2011, Physics and Chemistry of the Earth, Parts A/B/C, 87-88, 50–59, doi:10.1016/j.pce.2015.07.010, 2015.

Miehe, G., Schlütz, F., Miehe, S., Opgenoorth, L., Cermak, J., Samiya, R., Jäger, E. J., and Wesche, K.: Mountain forest islands and Holocene environmental changes in Central Asia: A case study from the southern Gobi Altay, Mongolia, Palaeogeogr. Palaeoclimatol. Palaeoecol., 250, 150–166, doi:10.1016/j.palaeo.2007.03.022, 2007.

Mukhortova, L., Schepaschenko, D., Shvidenko, A., McCallum, I., and Kraxner, F.: Soil contribution to carbon budget of Russian forests, Agr. Forest Meteorol., 200, 97–108, doi:10.1016/j.agrformet.2014.09.017, 2015.

Nyamjav, B., Goldammer, G.J., and Uibrig, H.: Fire situation in Mongolia, in: International Forest Fire News, 46–66, 2007.

Pan, Y., Birdsey, R. A., Fang, J., Houghton, R., Kauppi, P. E., Kurz, W. A., Phillips, O. L., Shvidenko, A., Lewis, S. L., Canadell, J. G., Ciais, P., Jackson, R. B., Pacala, S. W., McGuire, A. D., Piao, S., Rautiainen, A., Sitch, S., and Hayes, D.: A large and persistent carbon sink in the world's forests, Science (New York, N.Y.), 333, 988–993, doi:10.1126/science.1201609, 2011.

Poulter, B., Pederson, N., Liu, H., Zhu, Z., D'Arrigo, R., Ciais, P., Davi, N., Frank, D., Leland, C., Myneni, R., Piao, S., and Wang, T.: Recent trends in Inner Asian forest dynamics to temperature and precipitation indicate high sensitivity to climate change, Agr. Forest Meteorol., 178-179, 31–45, doi:10.1016/j.agrformet.2012.12.006, 2013.

Powell, S. L., Cohen, W. B., Healey, S. P., Kennedy, R. E., Moisen, G. G., Pierce, K. B., and Ohmann, J. L.: Quantification of live aboveground forest biomass dynamics with Landsat time-series and field inventory data: A comparison of empirical modeling approaches, Remote Sens. Environ., 114, 1053–1068, doi:10.1016/j.rse.2009.12.018, 2010.

Richter, H., Haase, G., and Barthel, H.: Die Golezterrassen, Petermanns Geographische Mitteilungen, 107, 183–192, 1963.

Rodríguez-Veiga, P., Quegan, S., Carreiras, J., Persson, H. J., Fransson, J. E.S., Hoscilo, A., Ziółkowski, D., Stereńczak, K., Lohberger, S., Stängel, M., Berninger, A., Siegert, F., Avitabile, V., Herold, M., Mermoz, S., Bouvet, A., Le Toan, T., Carvalhais, N., Santoro, M., Cartus, O., Rauste, Y., Mathieu, R., Asner, G. P., Thiel, C., Pathe, C., Schmullius, C., Seifert, F. M., Tansey, K., and Balzter, H.: Forest biomass retrieval approaches from earth observation in different biomes, Int. J. Appl. Earth Obs., 77, 53–68, doi:10.1016/j.jag.2018.12.008, 2019.

Rodríguez-Veiga, P., Wheeler, J., Louis, V., Tansey, K., and Balzter, H.: Quantifying Forest Biomass Carbon Stocks From Space, Curr. Forestry Rep., 3, 1–18, doi:10.1007/s40725-017-0052-5, 2017.

Schlütz, F., Dulamsuren, C., Wieckowska, M., Mühlenberg, M., and Hauck, M.: Late Holocene vegetation history suggests natural origin of steppes in the northern Mongolian mountain taiga, Palaeogeogr. Palaeoclimatol. Palaeoecol., 261, 203–217, doi:10.1016/j.palaeo.2007.12.012, 2008.

Shvidenko, A. Z. and Schepaschenko, D. G.: Carbon balance of Russian forests, Siberian Forest Journal, 1, 69–92, 2014.

Sommer, M. and Treter, U.: Die Lärchenwälder der Gebirgswaldsteppe in den Randgebieten des Uvs Nuur- Beckens, Die Erde, 130, 173–188, 1999.

Sugimoto, A., Yanagisawa, N., Naito, D., Fujita, N., and Maximov, T. C.: Importance of permafrost as a source of water for plants in east Siberian taiga, Ecol. Res., 17, 493–503, doi:10.1046/j.1440-1703.2002.00506.x, 2002.

Tchebakova, N. M., Parfenova, E., and Soja, A. J.: The effects of climate, permafrost and fire on vegetation change in Siberia in a changing climate, Environ. Res. Lett., 4, 45013, doi:10.1088/1748-9326/4/4/045013, 2009.

Thurner, M., Beer, C., Santoro, M., Carvalhais, N., Wutzler, T., Schepaschenko, D., Shvidenko, A., Kompter, E., Ahrens, B., Levick, S. R., and Schmullius, C.: Carbon stock and density of northern boreal and temperate forests, Global Ecol. Biogeogr., 23, 297–310, doi:10.1111/geb.12125, 2014.

Treter, U.: Gebirgs-Waldsteppe in der Mongolei, Geographische Rundschau, 48, 655–661, 1996.

Tsogtbaatar, J.: Deforestation and reforestation needs in Mongolia, Forest Ecol. Manag., 201, 57–63, doi:10.1016/j.foreco.2004.06.011, 2004.

Umbanhowar, C. E., Shinneman, A. L.C., Tserenkhand, G., Hammon, E. R., Lor, P., and Nail, K.: Regional fire history based on charcoal analysis of sediments from nine lakes in western Mongolia, Holocene, 19, 611–624, doi:10.1177/0959683609104039, 2009.

Unkelbach, J., Dulamsuren, C., Punsalpaamuu, G., Saindovdon, D., and Behling, H.: Late Holocene vegetation, climate, human and fire history of the forest-steppe-ecosystem inferred from core G2-A in the 'Altai Tavan Bogd' conservation area in Mongolia, Veget. Hist. Archaeobot., 27, 665–677, doi:10.1007/s00334-017-0664-5, 2017.

Unkelbach, J., Kashima, K., Enters, D., Dulamsuren, C., Punsalpaamuu, G., and Behling, H.: Late Holocene (Meghalayan) palaeoenvironmental evolution inferred from multi-proxy-studies of

https://doi.org/10.5194/bg-2020-13
Preprint. Discussion started: 3 March 2020

lacustrine sediments from the Dayan Nuur region of Mongolia, Palaeogeogr. Palaeoclimatol. Palaeoecol., 530, 1–14, doi:10.1016/j.palaeo.2019.05.021, 2019.

Vandandorj, S., Gantsetseg, B., and Boldgiv, B.: Spatial and temporal variability in vegetation cover of Mongolia and its implications, J. Arid Land, 7, 450–461, doi:10.1007/s40333-015-0001-8, 2015.

Yang, Y., Wang, Z., Li, J., Gang, C., Zhang, Y., Zhang, Y., Odeh, I., and Qi, J.: Comparative assessment of grassland degradation dynamics in response to climate variation and human activities in China, Mongolia, Pakistan and Uzbekistan from 2000 to 2013, J. Arid Environ., 135, 164–172, doi:10.1016/j.jaridenv.2016.09.004, 2016.